Enhancing hardness and wear behaviour of AA6061 reinforced with zirconium nitride through TOPSIS approach

Ganesan Kanmani[1] (iD), Viyat Varun Upadhyay[2], Sathish Kannan[3], Manzoore Elahi Mohammad Soudagar[4,5]

[1]Annai Mira College of Engineering and Technology, Department of Mechanical Engineering. Arappakkam, Ranipet, 632517, Tamil Nadu, India.

[2]GLA University, Department of Mechanical Engineering. Mathura, 281406, Uttar Pradesh, India.

[3]Saveetha University, Saveetha Institute of Medical and Technical Sciences, Saveetha School of Engineering, Department of VLSI Microelectronics. Chennai, 602105, Tamil Nadu, India.

[4]Chitkara University, Chitkara University Institute of Engineering and Technology, Centre for Research Impact and Outcome. Rajpura, 140401, Punjab, India.

[5]Lovely Professional University, Division of Research and Development, Phagwara 144411, Punjab, India.

e-mail: kanmani.phd@hotmail.com, viyat.upadhyay@gla.ac.in, sathishk.dr@outlook.com, me.soudagar@gmail.com

ABSTRACT

Aluminum matrix composites (AMCs) materials are highly valued in the aerospace and automotive industries for their exceptional characteristics. Zirconium nitride (ZrN) particles were used to reinforce aluminium alloy 6061(AA6061) to enhance the hardness and wear performance. Here the stir casting method is used to create four different composites with different amounts of ZrN particles (6, 12, and 18 wt.%). Using a Brinell hardness tester, the composites bearing the AA6061/12 wt.% ZrN formula achieved the highest recorded hardness value. Accordingly, these AA6061/12 wt.% ZrN composites were subjected to a tribological analysis. We conducted the trials with load (A), sliding speed (B), sliding distance (C) as the wear parameters. In order to determine the best parameter settings for attaining the minimum wear rate (Wr) and friction coefficient (COF), the TOPSIS method was used. Findings indicated that for 'A' = 18 N, 'B' = 2 m/s, 'C' = 1200 m, the COF and minimum Wr were achieved. The Analysis of Variance (ANOVA) data showed that factor 'A' contributed 45.43% of the total, with factor 'B' coming in second at 18.02%.

Keywords: AA6061; Composites; Hardness; Stir Casting; TOPSIS; Wear; Zirconium Nitride.

1. INTRODUCTION

Composite materials are gaining more and more popularity among consumers. When designing new goods, engineers often choose to use aluminium metal matrix composites (AMMCs) instead of unreinforced alloys because of the significant performance improvements they provide. Because of its exceptional qualities, including high strength-to-weight ratio, hardness, stiffness, and increased resistance to corrosion and wear. AMMCs find application in the aerospace, marine, automotive, and defence sectors [1]. By mixing two or more parts, with the matrix material serving as the major component and the reinforcement serving as the minor component, the properties can be customized. According to authors, the matrix material's properties are changed when reinforcements, with particles, were introduced [2, 3]. The low coefficient of thermal expansion, increased strength, hardness of ceramics such as oxides, nitrides and carbides make them ideal reinforcements for AMMCs. The incorporation of these reinforcements, the composites are able to accomplish properties that are not attainable with monolithic alloys [4]. Processing methods like stir casting, infiltration, and powder metallurgy, etc., typically determine the characteristics of AMMCs. As a result, producing an AMMCs isotropic product with a uniform delivery of reinforcing particles while keeping production costs low is of paramount importance. According to researchers stir casting is an affordable method that can create a homogeneous dispersion of particles compared to other production techniques for variety of alloys [5, 6]. Slag formation and porosity caused by the high temperatures involved are the drawbacks of the stir casting process. But, because of its adaptability and good range of cost, this method can be used widely [7]. The properties of AA6061 composites filled with various ceramics were investigated in a study [8, 9]. The researchers found mechanical and thermal properties were significantly enhanced as the ZrN content increased in the composites by synthesizing with two

different processes signifying their prospective for assorted engineering applications [10–12]. It was clear that the incorporation of titanium di oxide (TiO_2) greatly improved the hardness and reduced Wr. Researchers created Al6061/titanium diboride/Silicon carbide (SiC) hybrid composites and found that adding reinforcing particles greatly increased the composites' hardness and tensile strength [13]. According to authors who investigated the mechanical behaviours of AA6061/Zirconium di boride metal matrix composites, these composites outperformed the base alloy in terms of mechanical capabilities, and they also demonstrated that, with the right stir casting settings, a homogenous distribution could be attained [14]. The researchers found that SiC increased the hardness of composites made of aluminum and that the composites' Wr decreased as an oxide layer formed [15]. Researchers created AMMCs that were reinforced with different concentrations of silicon nitride (Si_3N_4) [16, 17]. According to their findings, adding Si_3N_4 enhances mechanical characteristics and reduces wear loss by 12 wt.%. When contrasted with the heat-treated AA6061 base alloy, the Si_3N_4 AMMCs was significantly lower. The mechanical and tribological behaviour of AMMCs reinforced with hybrid particles manufactured by stir casting were investigated [18].

Based on their findings, it is clear that adding particles enhances hardness and decreases wear loss. In their study on TiO_2 incorporated composites, authors found that load is the main determinant in lowering Wr and COF, after controlling for sliding velocity and distance [19]. The wear behaviour of $AA2219/ZrB_2$ composites were studied by authors using the Taguchi method for the wear rate [20]. The researchers found that the velocity and load had the maximum effect on the wear rate. Predicting the tribological behaviour and hardness behaviour of Aluminium matrix composites is a critical procedure that relies on additional parameters like 'A', 'B', and 'C,' as we learned from the many previous studies. Technique for order performance by similarity to ideal solution (TOPSIS) validated the ideal parameter arrangement, suggesting that approaches are very reliable for optimizing tribological features [21]. To determine the wear properties of aluminium composites, a comprehensive statistical evaluation is crucial. Therefore, this study set out to determine the best conditions for wear parameters to achieve the wear rate and friction coefficient for the suggested composites using TOPSIS method, as well as to examine the effect of ZrN content on hardness for AMMCs synthesized by the stir casting.

2. MATERIALS AND METHODS

2.1. Experimental details

Figure 1 displays the experimental plan of the investigation made for this research. In this work, ZrN with mean particle size of 30 μm was used as a matrix. AA6061 was also considered as it is most important in the aerospace and automotive sectors for the creation of shafts and gears, bicycle frames, transportation fittings,
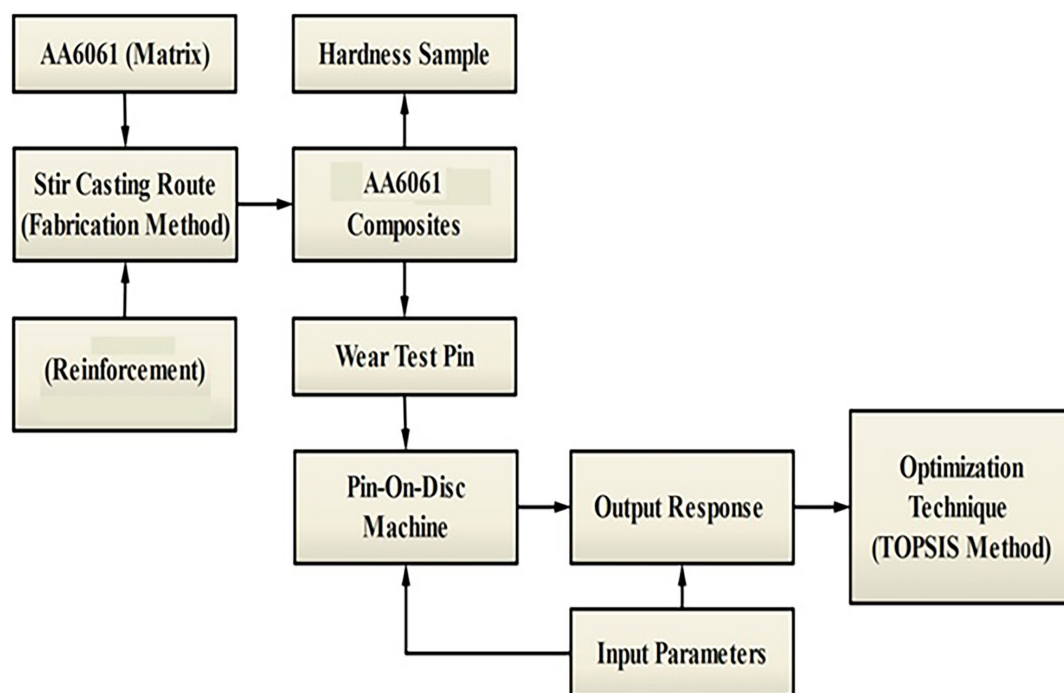

Figure 1: Experimental plan of present investigation.

missile components, and defence uses owing to its high toughness, natural aging properties, and strength-to-weight ratio [22, 23]. Copper = 1.42, Zinc = 5.4, Magnesium = 2.42, Chromium = 0.21, Iron = 0.42, Manganese = 0.12, Silicon = 0.13, and balance composition of Aluminium (wt.%). As casted AA6061, AA6061/6wt.% ZrN, AA6061/12 wt.% ZrN, and AA6061/18 wt.% ZrN were the four composite specimens that were created by adjusting the weight percent of ZrN particles. An electric furnace with separate stirrer was utilized to create the composite samples. An electric furnace was utilized to melt AA6061 ingots in graphite crucible starting at 800°C and bringing the temperature down to 650°C. In a similar vein, molten AA6061 was wettable on ZrN particles that had been warmed at 250°C to eliminate moisture. A motorized agitator was utilized to continuously agitate the molten AA6061 at 200 rpm. The next step was to gradually incorporate the warmed ZrN particles into the AA6061 pool using the vortex. To ensure that the particles in the AA6061 pool were evenly distributed, the mixture was continuously agitated at 250 rpm for 20 minutes. Immediately after churning, the warmed steel die was used to pour the slurry.

The hardness of the various composite specimens that were manufactured was measured utilizing the Brinell hardness test, with the ASTM E18 standard serving as a reference with the sample size of 10 mm width, 10 mm height and 10 mm length. The hardness value was used to choose the composite sample for the tribological behavior experiments. In many cases, materials with a high hardness also have a high resistance to wear. Therefore, in order to analyze tribological parameters like Wr and COF, the specimen was chosen for its higher hardness. Under dry sliding conditions, at room temperature and 50% humidity, a pin on disc tribometer was utilised to run the wear test. The ASTM G-99 standard was used as a guide to create the test pins, which were wire-cut electric discharge machined to 12 mm dia and 32 mm length. The Wr and COF are typically controlled by three variables: Load (A), Sliding Speed (B) and Sliding distance (C) [24]. For that reason, Table 1 contains these elements, which are considered as the input parameters. The studies were conducted utilizing a L9 (3³) orthogonal array displayed in Table 1, according to the settings that were selected. Equations (1) and (2) are utilized to measure the Wear rate and Friction Coefficient after the test [25].

$$Wr = (mm^3/m) = (\Delta m/\rho)/D \tag{1}$$

$$COF, \mu = F_T / F_N \tag{2}$$

The variables Δm (grams), D (slide distance, m), FT (tangential force, N), the composite density ρ, is given by g/mm³, and FN (normal force, N) are defined.

2.2. Optimization using TOPSIS technique

To address issues with multi-criteria decision-making (MCDM), this approach in used as presented by [26, 27]. Researchers employ maximum likelihood decision-making techniques to tackle multi-objective problems, with the goal of identification the optimal parameters from a set of possible values [28]. TOPSIS is used to optimize the parameters for wear control based on the estimated coefficient of friction and wear rate in this investigation. The TOPSIS algorithm chooses the optimal solution by comparing its distance to both positive and negative solutions. To determine the most optimal parameter settings, it is necessary to adhere to the following processes.

Table 1: Experimental results for the L9 (3³) array table.

S. No	A (N)	B (m/s)	C (m)	Wr (mm³/m)	COF
1	12	2	600	0.00702	0.57
2	12	4	1200	0.006	0.571
3	12	6	1800	0.00581	0.618
4	18	2	1200	0.00417	0.575
5	18	4	1800	0.00664	0.687
6	18	6	600	0.00921	0.662
7	24	2	1800	0.0073	0.724
8	24	4	600	0.00957	0.619
9	24	6	1200	0.00739	0.838

Step 1: To begin, with m options and n characteristics, the following is the formulation of the decision matrix D_{max}:

$$D = \begin{bmatrix} X_{11} & X_{12} & \cdots & \cdots & X_{1j} \\ X_{21} & X_{22} & \cdots & \cdots & X_{2n} \\ \cdots & \cdots & \cdots & \cdots & \cdots \\ X_{i1} & X_{i2} & \cdots & X_{ij} & X_{in} \\ \cdots & \cdots & \cdots & \cdots & \cdots \\ X_{m1} & X_{m2} & \cdots & X_{mj} & X_{mn} \end{bmatrix}$$

Step 2: Equation (3) is used to normalize the values that are produced by the decision matrix, denoted as (r_{ij}) Click or tap here to enter text.

$$r_{ij} = \frac{x_{ij}}{\sqrt{\sum_{i=1}^{m} x_{ij}^2}} \tag{3}$$

Step 3: Multiplying the normalized value by the weights assigned to each response yields the weighted normalized matrix (WNM), as shown in Equation (4).

$$v_{ij} = r_{ij} \times w_j \tag{4}$$

The weighted normalized matrix was displayed in Table 2.

Step 4: Equations (5) and (6) are used to find positive solution and negative solution (A⁻).

$$A^+ = \left\{ \sum_{i=1}^{max} v_{ij} / j \in J, \sum_{i=1}^{min} v_{ij} / j \in J' \right\} \tag{5}$$

$$A^- = \left\{ \sum_{i=1}^{min} v_{ij} / j \in J, \sum_{i=1}^{max} v_{ij} / j \in J' \right\} \tag{6}$$

J' – is linked to the non-benefit parameters while j is linked to the benefit parameters.

Step 5: Equations (7) and (8) utilize to find the separation measure for positive ideal solution and negative ideal solution:

$$S_i^+ = \sqrt{\sum_{j=1}^{n} (v_{ij} - A^+)^2}, \; i = 1, 2, \cdots, m. \tag{7}$$

$$S_i^- = \sqrt{\sum_{j=1}^{n} (v_{ij} - A^-)^2}, \; i = 1, 2, \cdots, m. \tag{8}$$

Table 2: WNM and normalized matrix.

Exp.No.	WNM		NORMALIZED MATRIX	
	Wr	**COF**	**Wr**	**COF**
1	0.0198	0.1664	0.0395	0.3329
2	0.0169	0.1667	0.0338	0.3335
3	0.0164	0.1805	0.0327	0.3609
4	0.0117	0.1679	0.0235	0.3358
5	0.0187	0.2006	0.0374	0.4012
6	0.0259	0.1933	0.0518	0.3866
7	0.0206	0.2114	0.0411	0.4228
8	0.0269	0.1808	0.0539	0.3615
9	0.0208	0.2447	0.0416	0.4894

Table 3: Measure of separation and relative proximity closeness.

EXP. NO.	SEPARATION MEASURE		RELATIVE CLOSENESS
	S_i^+	S_i^-	C_i
1	0.0072	0.0787	0.9165
2	0.0100	0.0781	0.8861
3	0.0176	0.0644	0.7857
4	0.0153	0.0768	0.8340
5	0.0351	0.0446	0.5595
6	0.0269	0.0533	0.6648
7	0.0454	0.0344	0.4313
8	0.0143	0.0657	0.8212
9	0.0785	0.0091	0.1035
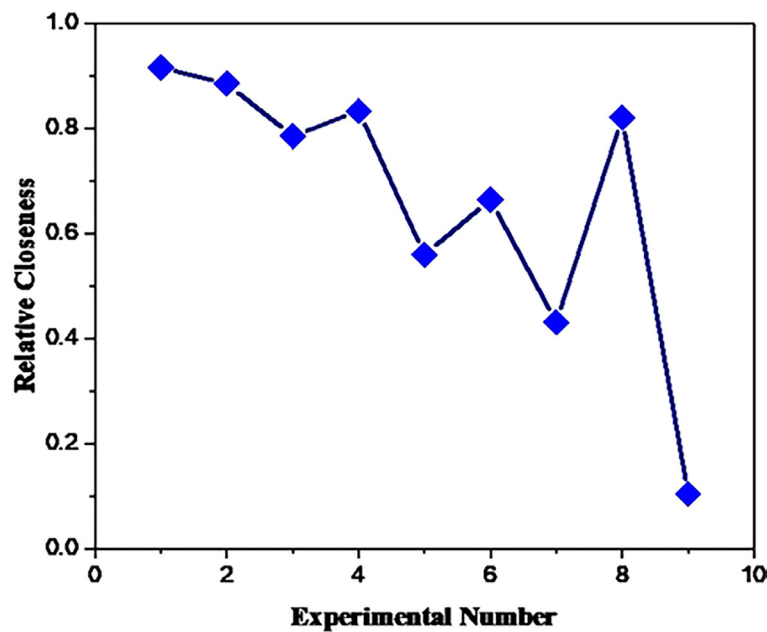
Figure 2: Plot of rank for the relative closeness.

Step 6: Equation (9) is used to determine how near each alternative is to the ideal answer, denoted as (C_i)

$$C_i = \frac{S_i^-}{S_i^+ + S_i^-} \tag{9}$$

Table 3 displays the computed distances and relative proximity.

Step 7: Put the degree of proximity in descending order. The highest rank is selected to obtain the best possible parameters. The ranked plot of the calculated relative proximity (C_j) is displayed in Figure 2. Results show that Ex. No. 1 has a closer relationship to the ideal combination of control parameters for minimizing Wr and COF with a relative proximity of 0.9165.

3. RESULTS AND DISCUSSIONS

3.1. Impact of ZrN particles on hardness

Hardness measurements taken at different points in the composite examples are shown graphically in Figure 3. In comparison to the other three composites, the AA6061/12 wt.% ZrN composite exhibits the best hardness and the least scatter in the measured spots. The composite's total hardness is increased when the hard reinforcement
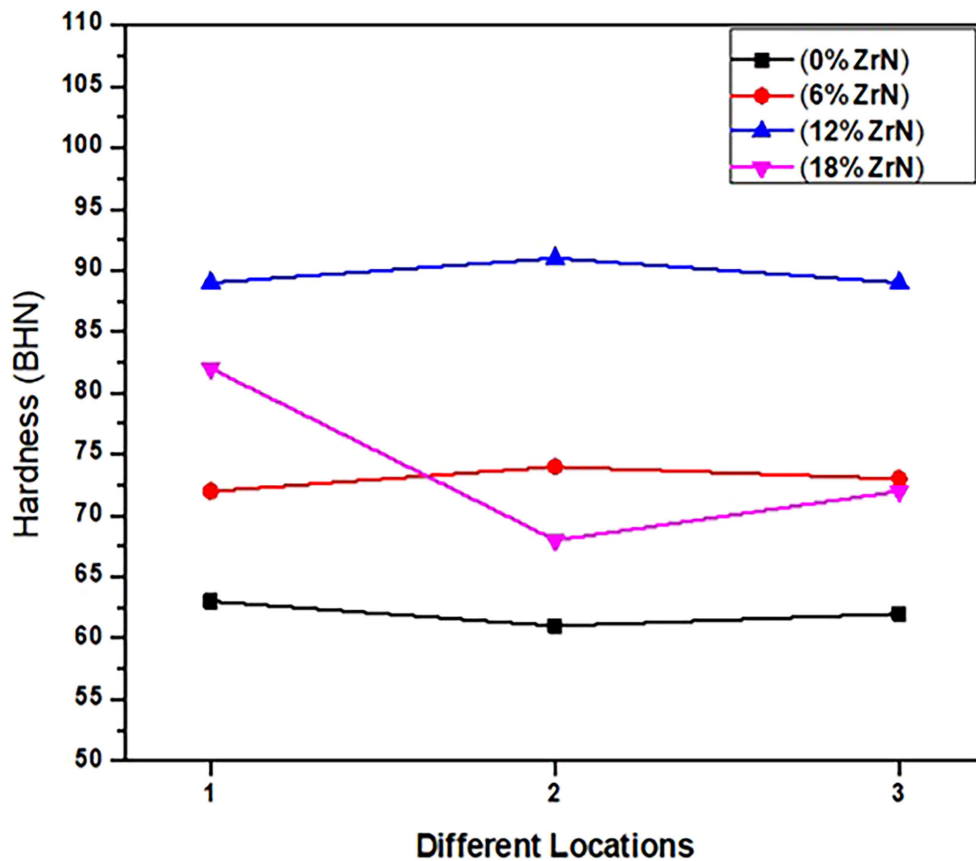
Figure 3: Brinell hardness of composites.

is added to the ductile matrix. The results with AA6061/18 wt.% ZrN likewise show peaks and valleys. Maximum hardness is produced by agglomerated reinforcing particles, as indicated by the peak, while the absence of reinforcing particles at that position is shown by the valley in AA6061/18wt.% ZrN. This shows that the reinforcing particles introduced into the AA6061/18wt.% ZrN are not uniformly distributed and it also shows that increasing the reinforcement content beyond 12 wt.% causes the reinforcement particles to be poorly distributed in the matrix, which reduces the hardness. An increase in hardness of 45.6% is achieved in introducing the 12-weight percentage of zirconium nitride reinforcement in to the matrix AA6061.

3.2. Impact of parameters on wear behaviour

Finding the ideal input parameter values to achieve the minimum FC and Wr under dry sliding conditions was the primary goal of this work. Figure 4 displays the average relative proximity for all parameter settings. Figure 4 shows that relative closeness (Ci) is represented by the mean value on the y-axis and individual level parameters (A, B, and C) on the x-axis.

A higher relative proximity number typically indicates the best combination of parameters. The optimal stages of the control variables are the load (12 N), sliding speed (4 m/s), the sliding distance (600 m), as presented in Figure 4. Optimal conditions show that the minimum sliding speed and distance, rise in load causes wear loss to occur faster. Growing the sliding and load distance typically leads to more wear loss. This is because the abrasive particles are able to plow more material from the specimen surface as they penetrate deeper into the specimen. The AA6061/ZrN composites achieve their lowest Wr and COF under these conditions: initial load, sliding speed, and distance.

Mean relative closeness (Ci) responses for every stage of control parameters as illustrated in Table 4. It was clear from the table which control settings had the most impact on the lowest Wr and COF. Table 4 shows that the load (A) is the maximum important factor in determining lowest friction coefficient and Wear succeeded by sliding speed (B) and distance (C). The use of the ANOVA analysis guaranteed this finding. The ANOVA is a popular statistical method for studying the effect of variables on a response. After conducting a dry sliding wear test on the AA6061/12 wt.% ZrN composite, the use an ANOVA to determine the effect of three control parameters, 'A,' 'B,' and 'C' on the COF and Wr.
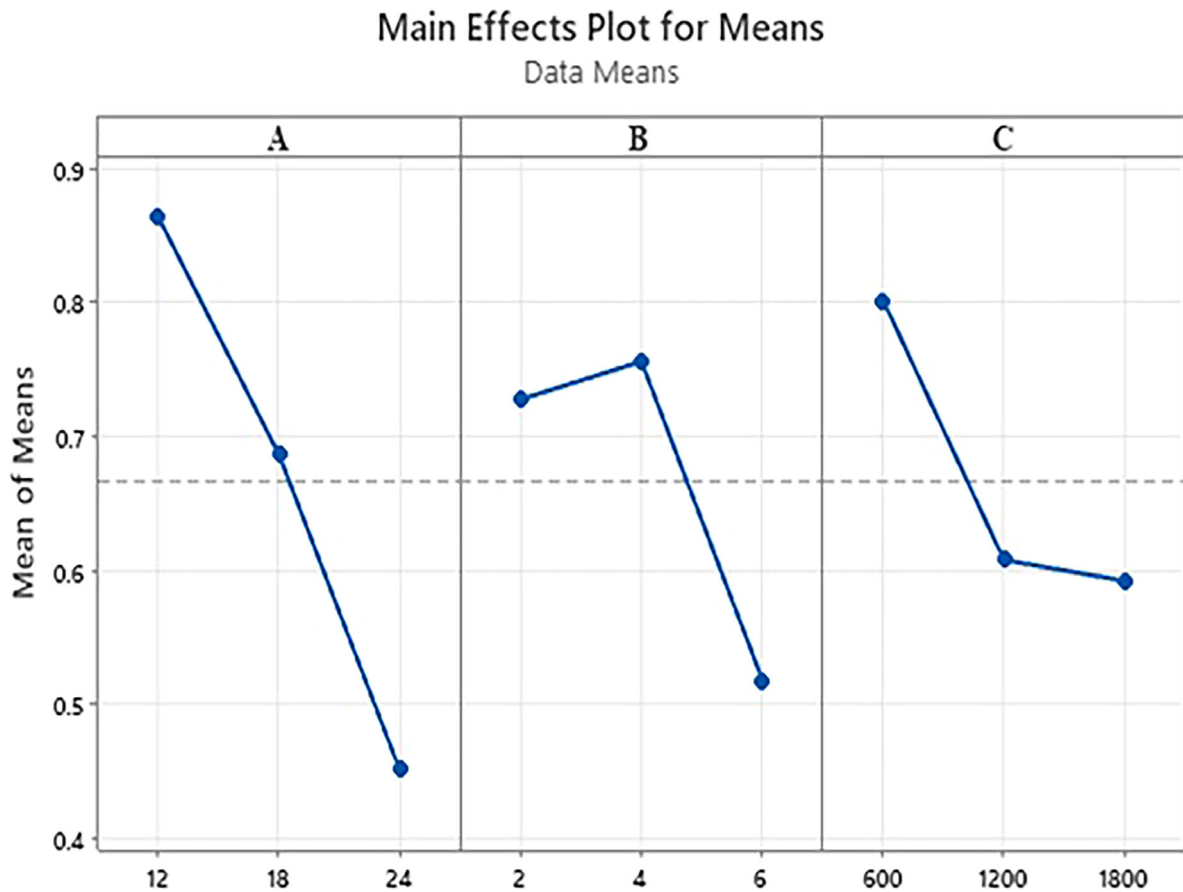
Main Effects Plot for Means
Data Means

Figure 4: Main effect plot for relative closeness.

Table 4: Means table for relative closeness.

LEVELS	A	B	C
1	0.8628	0.7272	0.8008
2	0.6861	0.7556	0.6078
3	0.4520	0.5180	0.5922
Delta	0.4108	0.2376	0.2087
Rank	1	2	3

Both the findings and the graphical depiction of the parameters' contributions are shown in Figure 5, with the former in Table 5. Figure 5 shows that out of the three prominent factors, the load accounts for the most (A = 45.43%), followed by the sliding speed (B = 18.02%) and the sliding distance (C = 14.45%). This work found the same thing when they tested AA6061- ZrN composites in dry sliding wear experiments; they found that the load is the significant impact on the tribological behaviour.

Figure 6 (a–c) displays the contour mapping of wear rate for AA6061 matrix composites evaluated with ZrN particles. The mapping is shown in relation to the control parameters: A, B, and C. Figure 6 (a) illustrates the combined impact of load and sliding speed on the wear. With the simultaneous rise in load and sliding speed, there was a prominent improvement in wear resistance. Nevertheless, the most minimal wear rate (0.0007 mm^3/m) is attained in conditions of initial speed and moderate load. At 4 m/s sliding speed, the maximum load of 24 N resulted in the maximum Wear rate (>0.009 mm^3/m). Figure 6 (b) demonstrates the impact of load and sliding distance on the wear resistance under examination. The data clearly indicates that the minimum wear rate occurs 1200 m sliding distance and 18 N load. However, when the load is increased at the first sliding distance of 1200 m, it results in a maximum Wr. This occurs because the maximum load exerts significant strain on the composite pin, resulting in an elevation of the weight ratio.
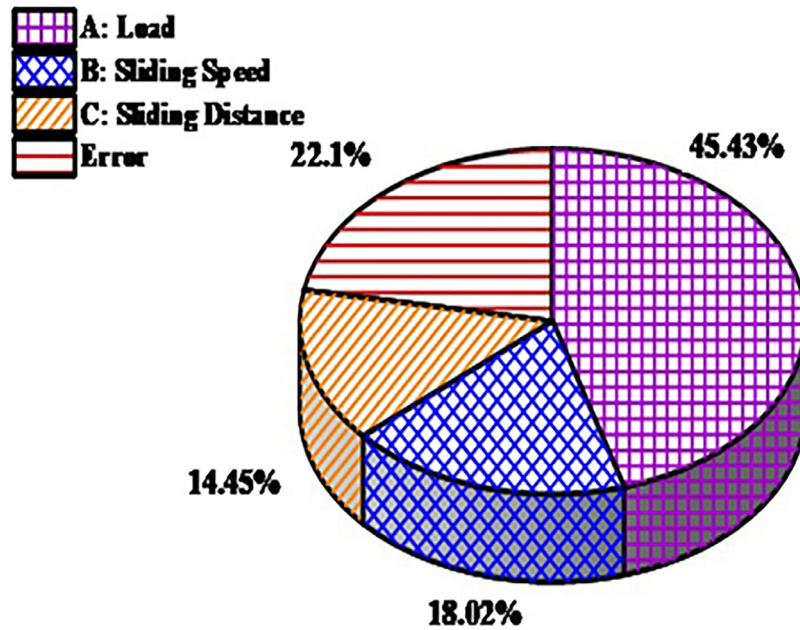
Figure 5: Plot of the various parameter's contributions.

Table 5: ANOVA for relative closeness.

SOURCE	DF	SEQ SS	ADJ MS	F-VALUE	P-VALUE
A	2	0.25473	0.12737	2.06	0.327
B	2	0.10103	0.05052	0.82	0.551
C	2	0.08103	0.04051	0.65	0.605
Error	2	0.12389	0.06195		
Total	8	0.56069			

Figure 6 (c) illustrates the impact of sliding speed and distance on the Wear rate. A 4 m/s decreased sliding speed combined with moderate sliding distance of 1200 m, results in a minimum wear rate. Likewise, the highest resistance to Wear rate was achieved when the sliding distance was the lowest (600 m) and the sliding speed was the highest (6 m·s⁻¹).

Figure 7 (a–c) shows contour mapping of COF for the AA6061/12 wt.% ZrN composites in relation to the wear control parameters. As displayed in Figure 7 (a-c), the variables A, B, and C represent the load, sliding speed, and distance, respectively. Figure 7 (a) shows the load-sliding speed interaction effect on friction coefficient of tested composite. At the minimum applied sliding speed of 2 m/s and load of 12 N, lowest COF (<0.45) was discovered, respectively. Concurrently, when both load and speed increased, the friction coefficient raised. The COF was larger (>0.70) when a 12 N load was applied with sliding speed of 6 m/s. The effect of load on COF as the function of sliding distance is displayed in Figure 7 (b). The intermediate stage of sliding distance (1200 m) with a weight ranging from 12 - 18N produced the lowest coefficient of friction (<0.45). In addition, the COF increases as the weight does, up to a max of 24 N, and when the sliding distance reaches 1200 m. At the dry sliding wear tests, Figure 7 (c) demonstrates how the COF of cast composite affected by sliding distance and sliding speed. Using a sliding speed of 2 m/s as well as medium sliding distance of 1200 m yields the lowest COF. At the medium sliding distance, though rise in sliding speed yields higher COF.

3.3. Confirmation test

The optimized parameters were considered in a confirmation experiment to validate the projected result of the tribological behaviour study of the AA6061/12 wt.% ZrN composite as displayed in Table 6. This was the last step in the process. Results showed that the experimental control parameters had a relative closeness (Ci) value
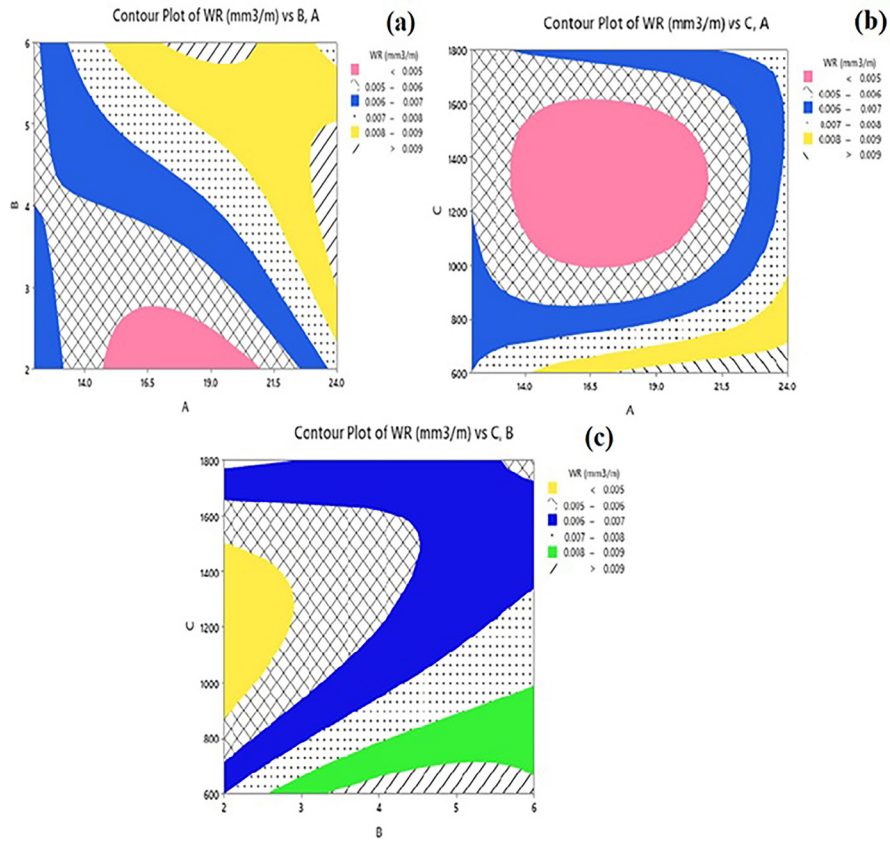
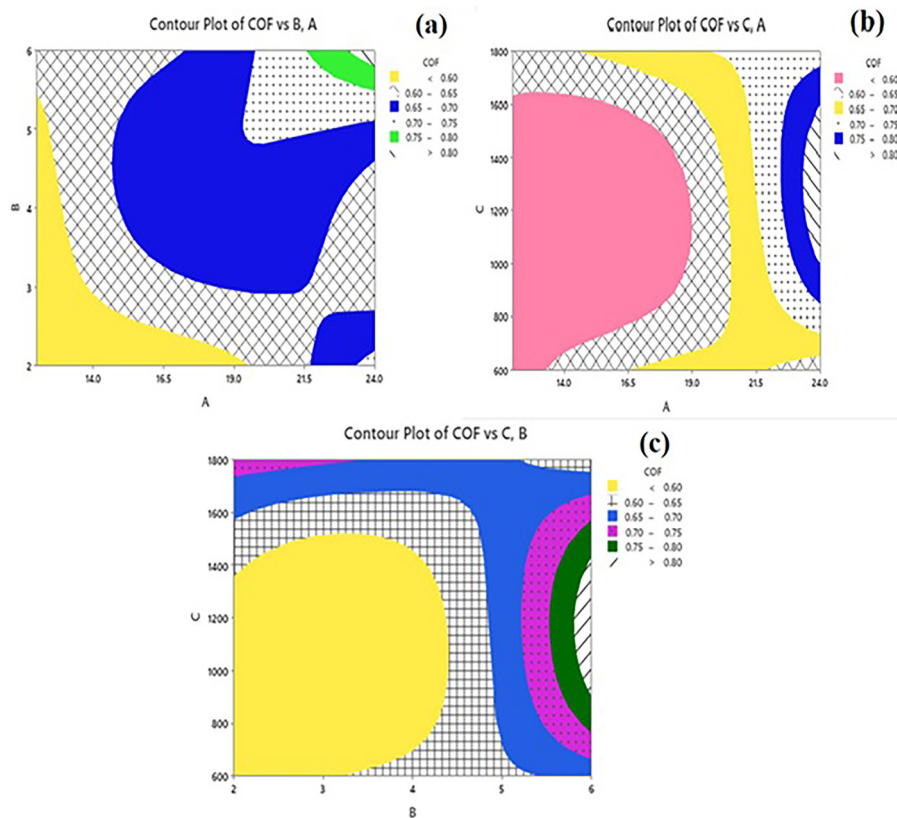**Figure 6:** Contour plot of Wr (a) A vs. B, (b) A vs. C (c) B vs. C.

Figure 7: Contour plot of coefficient of friction (a) A vs. B, (b) A vs. C (c) B vs. C.

Table 6: Confirmation experiments.

SETTING OF PARAMETER	OPTIMAL STAGE	WR (mm³/m)	COEFFICIENT OF FRICTION	RELATIVE CLOSENESS (C₁)	ERROR (%)
Experimental	$A_1B_1C_1$	0.00702	0.57	0.9165	1.18
Predicted	$A_1B_2C_1$	-	-	0.9283	

of 0.9165 and the projected control parameters had a value of 0.9283. An extremely minimum percentage error of 1.18% was achieved between the projected findings and experimental, indicating a very excellent correlation, according to the data.

4. CONCLUSIONS

Using the stir casting process, AA6061 matrix composites containing 6, 12, and 18 wt.% ZrN particles were successfully produced. The AA6061/12 wt.% ZrN composite achieved the highest hardness, according to measurements taken at various sites of the synthesized specimens. The hardness value was utilized to forecast the tribological behaviour under dry conditions using an AA6061/12 wt.% ZrN composite, and the TOPSIS technique was used to improve the control settings. According to the TOPSIS approach, the ideal control parameter values were determined to be A = 12 N, B = 4 m/s, and C = 600 m. The lowest Wr and COF were determined by doing an ANOVA to determine the relative importance of every process parameter. The analysis of variance displays that out of all the factors, load had the most impact (45.43%), followed by sliding speed (18.02%) and sliding distance (14.4%). The experimental responses were at a close range, with the predicted value having a minimal error of 1.18%. To find out how produced composites handle dry sliding wear, future scope will look into other optimization methods including ANN and GRA.

5. BIBLIOGRAPHY

[1]   SINGH, B., KUMAR, I., SAXENA, K.K., *et al.*, "A future prospects and current scenario of aluminium metal matrix composites characteristics", *Alexandria Engineering Journal*, v. 76, pp. 1–17, 2023. doi: http://doi.org/10.1016/j.aej.2023.06.028.

[2]   MOHANAVEL, V., RAJAN, K., RAVICHANDRAN, M., "Synthesis, characterization and properties of stir cast AA6351-aluminium nitride (AlN) composites", *Journal of Materials Research*, v. 31, n. 24, pp. 3824–3831, 2016. doi: http://doi.org/10.1557/jmr.2016.460.

[3]   KANTA DAS, D., CHANDRA MISHRA, P., SINGH, S., *et al.*, "Properties of ceramic-Reinforced aluminium matrix composites-a review", *International Journal of Mechanical and Materials Engineering*, v. 9, n. 12, pp. 1–16, 2014.

[4]   MOHANAVEL, V., RAVICHANDRAN, M., "Experimental investigation on mechanical properties of AA7075-AlN composites", *Materials Testing*, v. 61, n. 6, pp. 554–558, 2019. doi: http://doi.org/10.3139/120.111354.

[5]   KANNAN, C., RAMANUJAM, R., "Advanced liquid state processing techniques for ex-situ discontinuous particle reinforced nanocomposites: a review", *Science and Technology of Materials*, v. 30, n. 2, pp. 109–119, 2018. doi: http://doi.org/10.1016/j.stmat.2018.05.005.

[6]   SANKAR, T., MOHANAVEL, V., "Investigations on electrical discharge machining parameters of silicon nitride particles reinforced magnesium composites", *Matéria (Rio de Janeiro)*, v. 29, n. 4, pp. e20240615, 2024. doi: http://doi.org/10.1590/1517-7076-rmat-2024-0615.

[7]   SRINIVASAN, D., MEIGNANAMOORTHY, M., GACEM, A., *et al.*, "Tribological behavior of Al/Nanomagnesium/Aluminum nitride composite synthesized through liquid metallurgy technique", *Journal of Nanomaterials*, v. 2022, n. 1, pp. 7840939, 2022. doi: http://doi.org/10.1155/2022/7840939.

[8]   KAREEM, A., QUDEIRI, J.A., ABDUDEEN, A., *et al.*, "A review on AA 6061 metal matrix composites produced by stir casting", *Materials (Basel)*, v. 14, n. 1, pp. 175, 2021. doi: http://doi.org/10.3390/ma14010175. PubMed PMID: 33401426.

[9]   ARUNKUMAR, T., PAVANAN, V., MURUGESAN, V.A., *et al.*, "Influence of nanoparticles reinforcements on aluminium 6061 alloys fabricated via novel ultrasonic aided rheo-squeeze casting method", *Metals and Materials International*, v. 28, n. 1, pp. 145–154, 2022. doi: http://doi.org/10.1007/s12540-021-01036-0.

[10] SUVOROVA, V., VOLODKO, S., SUVOROV, D., *et al.*, "Enhanced microstructure and mechanical properties of ZrN-reinforced AlSi10Mg aluminum matrix composite", *Scientific Reports*, v. 14, n. 1, pp. 10152, 2024. doi: http://doi.org/10.1038/s41598-024-58614-6. PubMed PMID: 38698028.

[11] KRYUKOVA, O.G., KRYLOVA, T.A., "Synthesis of ZrN-Based Composites via Nitridation of Zircon+ Aluminum Mixtures in Combustion Mode", *Inorganic Materials*, v. 59, n. 4, pp. 417–422, 2023. doi: http://doi.org/10.1134/S0020168523040040.

[12] UL-HAMID, A., "Microstructure, properties and applications of Zr-carbide, Zr-nitride and Zr-carbonitride coatings: a review", *Materials Advances*, v. 1, n. 5, pp. 1012–1037, 2020. doi: http://doi.org/10.1039/D0MA00233J.

[13] HILLARY, J., RAMAMOORTHI, R., JOSEPH, J.D.J., *et al.*, "A study on microstructural effect and mechanical behaviour of Al6061-5% SiC-TiB$_2$ particulates reinforced hybrid metal matrix composites", *Journal of Composite Materials*, v. 54, n. 17, pp. 2327–2337, 2020. doi: http://doi.org/10.1177/0021998319894666.

[14] DINAHARAN, I., MURUGAN, N., "Microstructure and some properties of aluminium alloy AA6061 reinforced in situ formed zirconium diboride particulate stir cast composite", *International Journal of Cast Metals Research*, v. 27, n. 2, pp. 115–121, 2014. doi: http://doi.org/10.1179/1743133613Y.0000000097.

[15] PRABAHARAN, T., "Mechanical and tribological characterization of stir cast AA6061 T6-SiC composite", *Silicon*, v. 13, n. 12, pp. 4575–4582, 2021. doi: http://doi.org/10.1007/s12633-020-00781-y.

[16] ARYA, R.K., KUMAR, R., TELANG, A., *et al.*, "Effect of microstructure on mechanical behaviors of Al6061 metal matrix composite reinforced with Silicon Nitride (Si$_3$N$_4$) and Silicon Carbide (SiC) micro particles", *Silicon*, v. 15, n. 14, pp. 5911–5923, 2023. doi: http://doi.org/10.1007/s12633-023-02468-6.

[17] ARYA, R.K., KUMAR, R., TELANG, A.., "Influence of microstructure on tribological behaviors of Al6061 metal matrix composite reinforced with silicon nitride (Si$_3$N$_4$) and silicon carbide (SiC) micro particles", *Silicon*, v. 15, n. 9, pp. 3987–4001, 2023. doi: http://doi.org/10.1007/s12633-023-02309-6.

[18] YUVARAJ, N., KOLI, Y., VEDABOURISWARAN, G., *et al.*, "Mechanical and tribological properties of AA6061/SiC/Aloe Vera Powder Hybrid Al Composites Fabricated by Stir Casting", *Silicon*, v. 15, n. 5, pp. 2451–2465, 2023. doi: http://doi.org/10.1007/s12633-022-02168-7.

[19] BHARAT, N., BOSE, P.S.C.., "Optimizing the wear behaviour of AA7178 metal matrix composites reinforced with SiC and TiO2 nanoparticles: a comparative study using evolutionary and statistical methods", *Silicon*, v. 15, n. 11, pp. 4703–4719, 2023. doi: http://doi.org/10.1007/s12633-023-02395-6.

[20] LOGESH, K., MANOGAR, K., MAGESHKUMAR, K., *et al.*, "Optimization on wear characteristics of AA2219/Nano Zirconium Diboride composites through orthogonal array", *Interaction*, v. 245, n. 1, pp. 312, 2024. doi: http://doi.org/10.1007/s10751-024-02151-1.

[21] GAJEVIĆ, S., MARKOVIĆ, A., MILOJEVIĆ, S., *et al.*, "Multi-objective optimization of tribological characteristics for aluminum composite using Taguchi grey and TOPSIS approaches", *Lubricants (Basel, Switzerland)*, v. 12, n. 5, pp. 171, 2024. doi: http://doi.org/10.3390/lubricants12050171.

[22] UDOYE, N.E., FAYOMI, O.S.I., INEGBENEBOR, A.O., *et al.*, "Corrosion impact of AA6061/clay composite for industrial application", *AIP Conference Proceedings*, v. 2437, n. 1, pp. 020167, 2022. doi: http://doi.org/10.1063/5.0092584.

[23] LIU, J., TAN, M.-J., JARFORS, A.-E.-W., *et al.*, "Formability in AA5083 and AA6061 alloys for light weight applications", *Materials & Design*, v. 31, pp. S66–S70, 2010. doi: http://doi.org/10.1016/j.matdes.2009.10.052.

[24] ESSA, F.A., ELSHEIKH, A.H., YU, J., *et al.*, "Studies on the effect of applied load, sliding speed and temperature on the wear behavior of M50 steel reinforced with Al2O3 and/or graphene nanoparticles", *Journal of Materials Research and Technology*, v. 12, pp. 283–303, 2021.

[25] GHATREHSAMANI, S., AKBARZADEH, S., KHONSARI, M.M.., "Experimentally verified prediction of friction coefficient and wear rate during running-in dry contact", *Tribology International*, v. 170, pp. 107508, 2022. doi: http://doi.org/10.1016/j.triboint.2022.107508.

[26] DEY, A., SHRIVASTAV, M., KUMAR, P., "Optimum performance evaluation during machining of Al6061/cenosphere AMCs using TOPSIS and VIKOR based multi-criteria approach", *Proceedings of the Institution of Mechanical Engineers. Part B, Journal of Engineering Manufacture*, v. 235, n. 13, pp. 2174–2188, 2021. doi: http://doi.org/10.1177/0954405420958770.

[27] SEKAR, D., SUBBAIYAN, A., VIJAY, D., *et al.*, "Optimizing M-Sand material supplier selection in construction: a fuzzy multi-criteria decision-making approach", *Matéria (Rio de Janeiro)*, v. 29, n. 4, pp. e20240488, 2024. doi: http://doi.org/10.1590/1517-7076-rmat-2024-0488.

[28] SANJAY, M.R., MOHAMMAD, J., NAIDU, N.V.R., *et al.*, "TOPSIS method for selection of best composite laminate" In: Jawaid, M., Thariq, M., Saba, N. (eds), *Modelling of damage processes in biocomposites, fibre-reinforced composites and hybrid composites*. Kidlington: Woodhead Publishing, pp. 199–209, 2019. doi: http://doi.org/10.1016/B978-0-08-102289-4.00011-4.